

# Generation of dynamic temporal and spatial concentration gradients using microfluidic devices

Francis Lin,<sup>ab</sup> Wajeeh Saadi,<sup>b</sup> Seog Woo Rhee,<sup>b</sup> Shur-Jen Wang,<sup>b</sup> Sukant Mittal<sup>b</sup> and Noo Li Jeon<sup>\*b</sup>

<sup>a</sup> Department of Physics and Astronomy, University of California at Irvine, Irvine, CA 92697, USA

<sup>b</sup> Department of Biomedical Engineering, University of California at Irvine, Irvine, CA 92697, USA. E-mail: njeon@uci.edu; Fax: +1 949 824 9968; Tel: +1 949 824 9032

Received 28th October 2003, Accepted 6th February 2004  
First published as an Advance Article on the web 24th March 2004

This paper describes a microfluidic approach to generate dynamic temporal and spatial concentration gradients using a single microfluidic device. Compared to a previously described method that produced a single fixed gradient shape for each device, this approach combines a simple “mixer module” with gradient generating network to control and manipulate a number of different gradient shapes. The gradient profile is determined by the configuration of fluidic inputs as well as the design of microchannel network. By controlling the relative flow rates of the fluidic inputs using separate syringe pumps, the resulting composition of the inlets that feed the gradient generator can be dynamically controlled to generate temporal and spatial gradients. To demonstrate the concept and illustrate this approach, examples of devices that generate (1) temporal gradients of homogeneous concentrations, (2) linear gradients with dynamically controlled slope, baseline, and direction, and (3) nonlinear gradients with controlled nonlinearity are shown and their limitations are described.

## Introduction

Gradients of diffusible chemicals play an important role in many biological processes that involve directed cell migration or chemotaxis such as host defense,<sup>1,2</sup> wound healing,<sup>3</sup> embryogenesis<sup>4</sup> and cancer metastasis.<sup>5</sup> Traditionally, investigators have used Boyden chamber and under-agarose assays for cell migration research.<sup>6,7</sup> However, these conventional chemotaxis assays are limited by diffusion of molecules from a source to a sink and are not capable of generating and maintaining stable gradients. Recently, a microfluidic device that can generate well-defined stable concentration gradients of solutions has been reported.<sup>8,9</sup> This device has been used for investigating neutrophil chemotaxis in gradients of IL-8.<sup>10</sup> Main advantages of the microfluidics-based method over conventional chemotaxis assays are: (1) flexible gradient generation of various gradient shapes using different channel network designs and (2) stable gradients that can be maintained for long periods of time. Although useful for many applications, an important limitation of this method is that the gradient shape is fixed for each device, limiting application to a single static experiment. Moreover, this approach could not be applied for applications requiring temporal variations in concentration.<sup>11</sup> This paper describes a method of generating dynamically controlled temporal and spatial gradients using a single microfluidic device by integrating a simple “mixer module” with individually controlled fluidic inputs with the gradient generating network.

## Materials and methods

### Fabrication of microfluidic devices

Microfluidic devices were fabricated in poly(dimethylsiloxane) (PDMS) using soft lithography.<sup>8</sup> Briefly, a transparency mask with a minimum feature size of  $\sim 30 \mu\text{m}$  was printed using a high-resolution printer (Page One, CA) from a CAD file (Macromedia,

CA). The mask was used in 1 : 1 contact photolithography of SU-8 50 photoresist (MicroChem, MA) to generate a negative “master” consisting of  $\sim 100 \mu\text{m}$  high patterned photoresist on a Si wafer (Silicon Inc., ID). Positive replicas with embossed channels were fabricated by molding PDMS (Sylgard 184, Dow Corning, MI) against the master. Inlets and outlets (1 mm diameter holes) for the fluids were punched out using sharpened needle tips. The surface of the PDMS replica and a clean glass coverslide (Corning, NY) were treated with air plasma for 1 min (Model PDC-001, Harrick Scientific, NY) and brought together to form an irreversible seal.<sup>8</sup> This assembly produced the required system of microfluidic channels. Polyethylene tubing (PE-20, Becton Dickinson, MD) was inserted into the holes to make the fluidic connections. The tubing was then connected to syringe pumps to complete the fluidic device. Each mixing channel was  $\sim 50 \mu\text{m}$  wide and  $\sim 40 \text{mm}$  long (per generation) and the observation area was  $\sim 350 \mu\text{m}$  wide and  $\sim 12 \text{mm}$  long.

### Solution delivery

Buffer (PBS, Invitrogen, CA) and fluorescein isothiocyanate–dextran (FITC–Dextran) ( $5 \mu\text{M}$  in PBS, MW = 10 kDa, Sigma) were pumped into the microfluidic device using programmable syringe pumps (Model 50300, Kloeber, NV). Each input (that were connected to distinct inlets into the microfluidic network) was pumped with separate, independently controlled syringe pumps. Syringe pumps were controlled using a custom Labview program. The concentration of FITC–Dextran was calibrated using the standard method<sup>9</sup> for each experiment.

### Microscopy and analysis

Fluorescence micrographs of the observation area of the microfluidic device were taken using an inverted microscope (Nikon, NY) with a 20X objective and a digital CCD camera (Photometrics CoolSNAP, Roper Scientific, AZ). The microscope and CCD camera were controlled with MetaMorph (Universal Imaging, PA). Images were analysed using Scion Image (Scion Corp., MD) and Imaq Builder (National Instruments, TX) to obtain the gradient profile. Gradient profiles were simulated in a Labview program based on previous analysis.<sup>9</sup> Data from experiments and simulations were analysed using Sigma Plot (SPSS, IL) and Origin (OriginLab, MA). The discrepancy of the gradient profile between the experiments and simulations was obtained by calculating the percent difference of the fitting parameters.

## Results and discussion

### Temporal control of homogeneous concentrations

A simple microfluidic “mixer module” design (Fig. 1a) was designed to generate controlled mixtures of two fluidic inputs. Buffer and FITC–Dextran solutions, individually controlled by separate syringe pumps, were introduced into the microfluidic device *via* two inputs. In this example, the desired final concentra-



tion of FITC–Dextran was obtained by controlling the relative flow rates of each input. The mixing channel was 40 mm long, to allow complete mixing in the range of flow rates tested (total flow rate is  $1.6 \mu\text{l min}^{-1}$ , which yields the linear flow speed of approximately  $5.3 \text{ mm s}^{-1}$ ) for this experimental configuration.<sup>8</sup> If chaotic mixer design or other efficient mixing schemes are implemented, the length and time required to change concentrations can be significantly reduced.<sup>12</sup> The final concentration in the observation area, 40 mm downstream of the inputs, is spatially homogeneous. The final concentration is controlled by varying the ratio ( $k$ ) of buffer ( $V_{\text{buffer}}$ ) and FITC–Dextran ( $V_{\text{FITC-Dextran}}$ ) flow rates, where

$$k = \frac{V_{\text{Buffer}}}{V_{\text{FITC-Dextran}}} \quad (1)$$

If the portion of the mixing channel occupied by a fluidic input is proportional to its flow rate, the relationship between the normalized final concentration of FITC–Dextran ( $c$ ) in the observation channel and the flow rate ratio ( $k$ ) is given by

$$c = \frac{1}{1+k} \quad (2)$$

If the total flow rate in the observation channel is kept constant (as in this experiment),

$$V_{\text{Buffer}} + V_{\text{FITC-Dextran}} = V_0 \quad (3)$$

Then the flow rates of buffer and FITC–Dextran as a function of the normalized FITC–Dextran concentration  $c$ , and the total flow rate  $V_0$  can be readily determined.

$$V_{\text{FITC-Dextran}} = cV_0 \quad (4)$$

$$V_{\text{Buffer}} = (1-c)V_0$$

Since the FITC–Dextran concentrations for  $k = 0$  (FITC–Dextran only) and  $k = \infty$  (buffer only) are known, and their fluorescence intensity can be measured, we used these values as reference points to test the proposed mixing strategy by examining whether the relative fluorescence intensity is linearly proportional to the FITC–Dextran concentration at other  $k$  values. Plotting the normalized fluorescence intensity *versus* the normalized FITC–

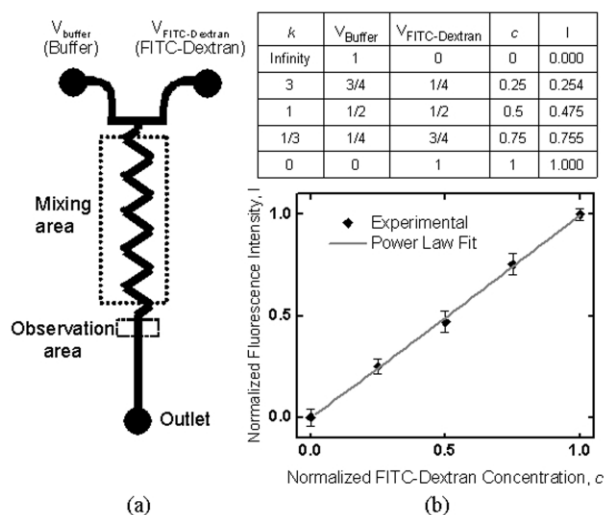


**Fig. 1** Two-input “mixer module”. (a) Design of the microfluidic chamber. Buffer and FITC–Dextran were infused into the top inputs and allowed to mix completely before reaching the observation area 40 mm downstream. The final concentration is controlled by the relative flow rates of buffer and FITC–Dextran, which were pumped by separate, independently controlled syringe pumps. (b) Normalized fluorescence intensity ( $I$ ) in the observation channel was measured at different FITC–Dextran concentrations ( $c$ ). Error bars indicate standard deviation. The table above the plot shows the flow rate ratio ( $k$ ), normalized flow rates of buffer and FITC–Dextran, and  $I$  in the observation channel as a function of FITC–Dextran concentration. The total flow rate was maintained at  $1.6 \mu\text{l min}^{-1}$ .

Dextran concentration gave a straight line, indicating that the strategy is valid (Fig. 1b).

Because the solution was pumped into the channel using syringe pumps driven by stepper-motors which controlled the flow rate by varying the time interval between steps, the mixing precision was limited by the pulsatile nature of the pumps. The experimental results showed that eqn. (2) is valid only under one of the following conditions:

- (1)  $k = 0$ , the buffer is stopped and the normalized FITC–Dextran concentration is 1;
- (2)  $k = \infty$ , the FITC–Dextran is stopped and the normalized FITC–Dextran concentration is 0;
- (3)  $0.1 \leq k \leq 9$ , the buffer and FITC–Dextran divide the mixing channel according to their flow rates and give the normalized FITC–Dextran concentration from eqn. (2).

For  $k < 0.1$ , except 0, the FITC–Dextran solution will occupy the entire channel for most of the time since its flow rate is much faster than the buffer’s. For  $k > 9$ , except infinity, the buffer will occupy the entire channel for most of the time since its flow rate is much faster than the FITC–Dextran’s. This range will vary if different total flow rates or different sizes of syringes are used. Pulse-free pumps or gravity-based pumps<sup>13</sup> may be used to overcome this limitation.

In addition to generating dynamic temporal gradients of uniform concentrations, this method can be used as a basic building block to generate dynamic spatial gradients as shown below.

### Generation of dynamic linear gradients

To generate dynamically controlled spatial and temporal linear gradients with varying slope, baseline, and direction, the outlet of the “mixer module” described in the previous section was connected to the inlets of a gradient generating device (Fig. 2a). It has been previously demonstrated that linear concentration gradients can be generated with a symmetric microchannel network with two inlets.<sup>8</sup> In this earlier device, the slope of the gradient was

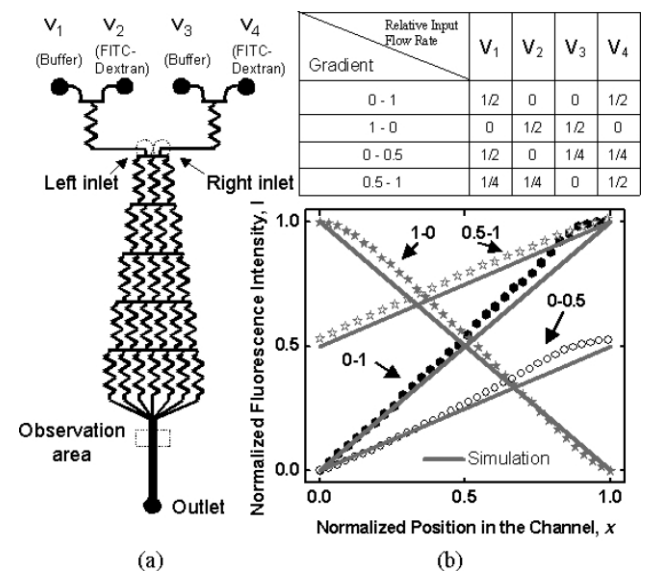


**Fig. 2** Generation of dynamic linear gradients. (a) Design of the microfluidic device. Two “mixer modules” were connected to a two-inlet gradient device that generates linear gradients. This device is capable of generating linear gradients of different slope, baseline, and direction. Furthermore, the gradients can be dynamically controlled during an experiment by simply changing the relative flow rates of buffer and FITC–Dextran into the “mixer modules”. (b) 0–1 (linear gradient from 0% to 100% FITC–Dextran), 0–0.5 (decrease the slope by 50%), 0.5–1 (increase the baseline to 50% FITC–Dextran), and 1–0 (change the direction from 0–100% FITC–Dextran to 100–0% FITC–Dextran) linear gradients across a  $350 \mu\text{m}$  channel were experimentally measured and compared with simulations. The table shows the normalized relative flow rates into each input ( $V_1, V_2, V_3, V_4$ ) used to generate different linear gradients. The total flow rate in the observation channel was maintained at  $3.2 \mu\text{l min}^{-1}$ .

determined by the difference between the concentrations of the chemical (FITC–Dextran) in the two inlets. For example, if the FITC–Dextran concentrations are 0% and 100% for the left inlet and right inlet respectively, a 0%–100% linear gradient can be generated in the observation area perpendicular to the flow streams.

The baseline concentration of the gradient in this earlier device was determined by the concentration of FITC–Dextran for each inlet. This configuration required that solutions with different FITC–Dextran concentrations be prepared separately to change the shape of the gradient. Here, a “mixer module” as described in the previous section (*i.e.*, a mixer with a buffer input and a FITC–Dextran input), was added to each inlet of the gradient generator (Fig. 2a). (Note that the 4 fluidic inputs controlled with separate syringe pumps were used to control the concentration of FITC–Dextran that was injected into the inlets.) By adjusting the relative flow rates of the buffer and the FITC–Dextran inputs, while maintaining constant total flow rate, the concentration of FITC–Dextran injected into each inlet can be dynamically varied to change the slope, the baseline, and the direction of the linear gradients.

The slope of the gradient was changed by varying the relative concentration of FITC–Dextran injected into the inlets. Keeping the left inlet constant, the slope can be changed by changing the concentration of FITC–Dextran into the right inlet. Here, linear gradients are represented by the normalized FITC–Dextran concentration change from the left edge to the right edge of a 350  $\mu\text{m}$  wide microchannel. For example, a 0–1 linear gradient (linear gradient of FITC–Dextran from 0% to 100%) is generated if the FITC–Dextran input for the left inlet and the buffer input for the right inlet are stopped (Fig. 2b). If both inputs for the right inlet are turned on with equal flow rates, the FITC–Dextran concentration in the right inlet is diluted by 50% ( $k = 1$ ), and a 0–0.5 linear gradient (0% to 50%) can be created. Thus lowering the effective concentration of FITC–Dextran injected into right inlet from 100% to 50% effectively changes the slope of the linear gradient (Fig. 2b).

Similarly, the baseline of the linear gradient can be varied by adjusting FITC–Dextran concentrations of each inlet independently. For instance, to form a 0.5–1 linear gradient, the FITC–Dextran input for the left inlet was diluted by 50% by the buffer input ( $k = 1$ ), and the buffer input for the right inlet was stopped, increasing the baseline of the gradient to 0.5 while maintaining the same slope as the 0–0.5 linear gradient (Fig. 2b). This is useful for experiments that require a background chemical concentration. Traditional methods of generating gradients, such as the Boyden chamber, are not capable of varying the baseline of the gradient because of their diffusive nature.

This device is also capable of dynamically reversing the gradient direction. For example, a 0–1 linear gradient can be changed to a 1–0 linear gradient by switching the on/off status of each input (Fig. 2b). More specifically, for a 0–1 linear gradient, the buffer input for the left inlet and the FITC–Dextran input for the right inlet were turned on, and the other two inputs were turned off. For a 1–0 linear gradient, the FITC–Dextran input for the left inlet and the buffer input for the right inlet were turned on, and the other two inputs were turned off instead.

Fig. 2b also shows the gradient profiles for each of the tested linear gradients, as generated by computer simulations. The linear gradients that can be generated by this method are limited by the possible FITC–Dextran concentrations from the “mixer modules”.

The total flow rate in the observation channel as well as in each inlet is kept constant. The importance of this feature will be discussed in the next section.

### Generation of dynamic nonlinear gradients

A three-inlet nonlinear spatial gradient generator has been demonstrated previously.<sup>8,9</sup> In that device, the gradient was

described by equation  $c = ax^b + O(x)$ , where  $c$  was the concentration,  $x$  was the position in the channel,  $a$  and  $b$  were the proportion coefficient and the power of the major term respectively, and  $O(x)$  represented the remaining terms. The nonlinearity (or power) of the gradient was modified by adjusting the relative chemical concentration of the middle inlet. To change the concentration of the middle inlet, the experiment had to be stopped and the solution being pumped into the inlets had to be manually replaced with another. This section describes the incorporation of the “mixer module” into the middle inlet to allow dynamic control of the nonlinearity of the gradient. A “mixer module” with a buffer input and a FITC–Dextran input was used (Fig. 3a). Our experimental results showed that the gradient profile is in the power law form,

$$c(x) = ax^b \quad (5)$$

where  $c$  is the normalized FITC–Dextran concentration as a function of the position ( $x$ ) in the observation channel (the origin is at the left edge of the channel), and is directly proportional to its fluorescence intensity;  $a$  and  $b$  are fitting parameters. The power  $b$  varies from  $\sim 0.5$  to  $\sim 2$ , depending on the FITC–Dextran concentration of the middle inlet, and is in agreement with simulations.

Fig. 3b shows both the experimental results and the computer simulations of various nonlinear gradients. The gradient profiles were simulated by calculating the spatial distribution of FITC–Dextran concentration resulting from the repeated splitting and mixing of FITC–Dextran and buffer from inlets and flowing through the microchannel network.

This demonstration illustrates the usefulness of combining “mixer modules” to dynamically generate different spatial gradients. More sophisticated devices can be designed by adding more “mixer modules” to control the gradient conditions with more flexibilities. For example, increasing the number of middle inlets

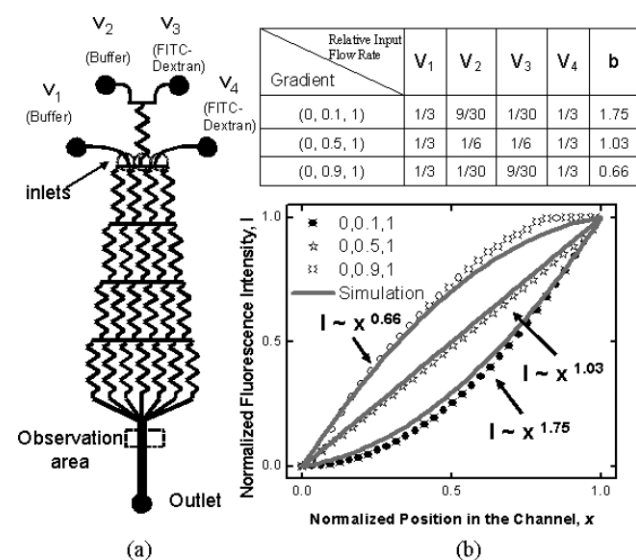


**Fig. 3** Generation of dynamic nonlinear gradients: (a) A “mixer module” was connected to the middle inlet of a three-inlet nonlinear gradient device. The concentration of FITC–Dextran was fixed at 0 and 1 for left and right inlets, respectively. Relative flow rates of FITC–Dextran and buffer were dynamically controlled to yield the appropriate concentration of FITC–Dextran in the middle inlet. This results in nonlinear gradients with different nonlinearity (the power  $b \approx 0.5$  and 2 for middle inlet concentrations of 1 and 0, respectively). Different middle inlet concentrations of FITC–Dextran yields different nonlinear gradients in the observation channel. (b) Nonlinear gradients are represented by the combination of three inlets concentrations (left, middle, right) and are in power law form ( $I = ax^b$ ). Fig. 3b shows gradient profiles of (0,0.1,1), (0,0.5,1), and (0,0.9,1) from the experiments and the simulations. The table shows the normalized input flow rates for different nonlinear gradients and the experimentally determined power of the gradients. Other nonlinear gradients from (0,0,1) to (0,1,1) were also tested (not shown) and were found to agree with the simulations. The total flow rate in this device was kept constant at 4.8  $\mu\text{l min}^{-1}$ .

with “mixer modules” of temporal concentration control can further increase the nonlinearity of the gradient.

We demonstrated that when two more middle inlets are added, the power can be as high as  $\sim 4.2$ . By manipulating the concentration in these inlets as described above, a wide range of gradient shapes can be obtained.

Fig. 4 shows the design of the simplified three-middle-inlet device and gradient profiles from both the experiment and the simulation when all the middle inlet concentrations are zero. This device can create a very steep gradient, but is different from the serial diluter shown in other studies<sup>14</sup> that can also generate steep gradients described by the equation  $c = a(\frac{x}{L})^x$ , where  $x = 0, 1, 2, 3, \dots$

Note that the dynamic nonlinear gradient generator is also capable of generating linear gradients when the middle inlets have the appropriate concentrations. For example, the gradient profile is linear when the normalized middle inlet concentration of FITC-Dextran is 0.5 in the three-inlet device (Fig. 3b). Using this approach, various types of gradients including homogeneous concentrations, linear and nonlinear gradients, can be conveniently generated in a single device.

Another advantage of this method is that since the total flow rate is kept constant, other experimental conditions such as shear stress, are not affected when the gradient is changed.

An average of 7% discrepancy between the experimental results and the computer simulations was observed. This was mainly caused by the pulsing of the flows, and can be reduced by using pulse-free pumps or gravity-based pumps.<sup>13</sup> The saturation of

fluorescence intensity near the edges of the channel also contributed to this deviation.

## Conclusion

This paper describes a simple microfluidics-based approach to generate dynamic temporal and spatial concentration gradients. The approach integrates two-input (inputs individually controlled by syringe pumps) mixers into the inlets of a gradient network device. By adjusting the relative flow rates of solutions delivered into the mixer, dynamic temporal gradients, linear gradients of different slope, baseline, and direction, and nonlinear gradients with different nonlinearity can be produced. Although the approach described in this paper can generate flexible shapes of gradients using a single microfluidic device, it requires integration of computer controlled syringe pumps that add complexity and limit some shapes due to pulsatile nature of the stepper-motor driven syringe pump. In spite of these limitations, the added flexibility in the gradient shape and capacity to generate dynamic temporal and spatial gradients will be broadly useful in many areas of applications where flexible gradient generations are needed. We are in the process of using the approach described in this report to investigate neutrophil and breast cancer cell migration.

## Acknowledgements

This research is supported by NSF (Grant No. DBI-0138055) and the U.S. Public Health Service-National Institutes of Health General Medical Science Grant (GM-66051).

## References

- 1 S. Zigmond, *J Cell Biol.*, 1981, **88**, 644–7.
- 2 S. Zigmond, *J Cell Biol.*, 1977, **75**, 606–16.
- 3 D. M. Knapp, E. F. Helou and R. T. Tranquillo, *Exp. Cell Res.*, 1999, **247**, 543–53.
- 4 T. N. Behar, A. E. Schaffner, C. A. Colton, R. Somogyi, Z. Olah, C. Lehel and J. L. Barker, *J. Neurosci.*, 1994, **14**, 29–38.
- 5 L. V. Dekker and A. W. Segal, *Science*, 2000, **287**, 982–3.
- 6 S. V. Boyden, *J. Exp. Med.*, 1962, **115**, 453–66.
- 7 R. D. Nelson, P. G. Quie and R. L. Simmons, *J. Immunol.*, 1975, **115**, 1650–6.
- 8 N. L. Jeon, S. K. W. Dertinger, D. T. Chiu, I. S. Choi, A. D. Stroock and G. M. Whitesides, *Langmuir*, 2000, **16**, 8311–6. \*This paper detailed the generation of microfluidic gradients.
- 9 K. W. S. Dertinger, D. T. Chiu, N. L. Jeon and G. M. Whitesides, *Anal. Chem.*, 2001, **73**, 1240–6. \*This paper also detailed the generation of microfluidic gradients.
- 10 N. L. Jeon, H. Baskaran, S. K. W. Dertinger, G. M. Whitesides, L. V. D. Water and M. Toner, *Nat. Biotechnol.*, 2002, **20**, 826–30.
- 11 S. Zigmond and S. J. Sullivan, *J. Cell Biol.*, 1979, **82**, 517–27.
- 12 A. D. Stroock, S. K. W. Dertinger, A. Ajdari, I. Mezic, H. A. Stone and G. M. Whitesides, *Science*, 2002, **295**, 647–51.
- 13 M. A. Unger, H. P. Chou, T. Thorsen, A. Scherer and S. R. Quake, *Science*, 2000, **288**, 113–6.
- 14 X. Jiang, J. M. K. Ng, A. D. Stroock, S. K. W. Dertinger and G. M. Whitesides, *J. Am. Chem. Soc.*, 2003, **125**, 5294–5.

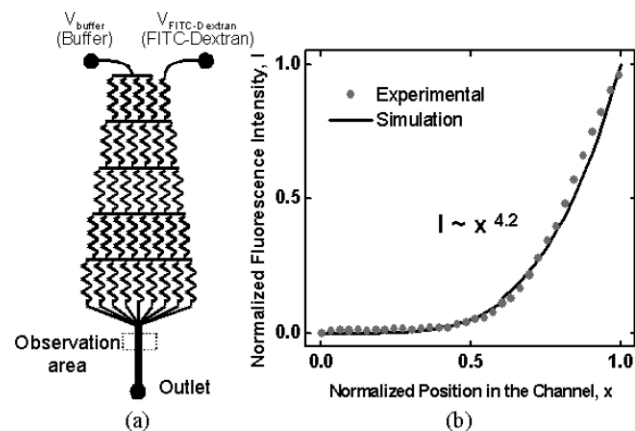


**Fig. 4** Generation of a nonlinear gradient with higher steepness: (a) Design of a simplified 3-middle-inlet microfluidic chamber. A buffer inlet splits into four sub-inlets to simplify the experimental setup. This is equivalent to a buffer inlet, three separate middle inlets and an FITC-Dextran inlet, with the concentrations (0, 0, 0, 0, 1). (b) Gradient profiles from the experiment and the simulation are shown ( $b \approx 4.2$ ). For the relative input flow rates,  $V_{\text{Buffer}} = 4V_{\text{FITC-Dextran}}$ . The total flow rate in the observation channel was maintained at  $4.0 \mu\text{l min}^{-1}$ .